Desalination and Water Treatment
www.deswater.com
doi: 10.5004/dwt.2017.20745

78 (2017) 273–280
June

Degradation of Acid Blue 113 by US/H_2O_2/Fe^{2+} and US/$S_2O_8^{2-}$/Fe^{2+} processes from aqueous solutions

Abdolmotaleb Seid-Mohammadi[a], Amir Shabanloo[a], Mehdi Fazlzadeh[b], Yousef Poureshgh[c,*]

[a]*Department of Environmental Health Engineering, School of Public Health, Hamadan University of Medical Sciences, Hamadan, Iran, Tel. +98 9181317314; email: sidmohammadi@umsha.ac.ir (A. Seid-Mohammadi), Tel. +98 9183786151; email: Shabanlo_a@yahoo.com (A. Shabanloo)*
[b]*Department of Environmental Health Engineering, School of Public Health, Ardabil University of Medical Sciences, Ardabil, Iran, Tel. +984515513428; email: m.fazlzadeh@gmail.com*
[c]*Department of Environmental Health Engineering, School of Public Health, Hamadan University of Medical Sciences, Hamadan, Iran, Tel. +989148092356; Fax: +984533512004; email: yusef.poureshg@gmail.com*

Received 30 June 2016; Accepted 21 March 2017

ABSTRACT

Azo dyes can lead to a number of problems in the environment due to the presence of benzene rings in their structure. Therefore, the removal of these pollutants is necessary before being discharged directly into the environment. This experimental study aimed to evaluate the degradation capability of Acid Blue 113 (AB113) by the ultrasound (US)/H_2O_2/Fe^{2+} and US/$S_2O_8^{2-}$/Fe^{2+} processes. The effects of variables like initial pH, Fe^{2+}, H_2O_2, and $S_2O_8^{2-}$ and initial AB113 concentrations on the removal efficiency were investigated using a 20-kHz batch ultrasound generator. The impact of aeration was also examined under optimum conditions; in addition, analysis of wavelength scan of AB113 dye was done. The results showed that the maximum rate of decolorization occurred at pH 3 for both processes. In US/H_2O_2/Fe^{2+} process, H_2O_2 (2.5 mM), Fe^{2+} (0.05 mM), and reaction time (45 min) were selected as the optimum conditions with a removal efficiency of 93.5%. Under the same conditions, 94.3% of the dye was removed via the US/$S_2O_8^{2-}$/Fe^{2+} process. Moreover, aeration decreased the efficiency for both processes. Further, aeration improved the efficiency of US waves used solely. The highest change in the UV–Vis spectrum of AB113 was observed for US/H_2O_2/Fe^{2+}, US/$S_2O_8^{2-}$/Fe^{2+}, $S_2O_8^{2-}$/Fe^{2+}, and H_2O_2/Fe^{2+}.

Keywords: Ultrasound; Hydrogen peroxide; Persulfate; Acid Blue 113 degradation

1. Introduction

Rapid development of the textile industry and extensive use of synthetic dyes in recent decades have introduced these dyes as a major source of water pollution [1,2]. Synthetic dyes are also extensively used in various industries such as leather, cosmetics, printing inks, foodstuffs, paper and plastics, and dyestuff production [3,4]. Annually, over 7 × 105 tons of dyestuff is produced worldwide; almost 10%–15% of the total amount of dyes used is found in the effluents disposed from such industries into the environment without any pretreatment [5]. Moreover, azo dyes comprise 70% of all produced dyes in the world. These dyes, due to the presence of azo groups (–N=N–) and aromatic rings in their structure, are degraded slowly in the environment and have toxic, mutagenic, and carcinogenic characteristics and impose aesthetic problems [6–8]. Therefore, the removal of these problematic pollutants has been one of the major concerns of environmental agencies [9].

Adsorption onto activated carbon, sedimentation, photodegradation, biodegradation, coagulation, and electrocoagulation are common methods for the successful

* Corresponding author.

treatment of colored wastewaters. Among these, adsorption onto activated carbon is an expensive and time-consuming method, which consequently does not yield a desirable and proper efficiency [10–12]. And oxidation by chlorine compounds produces harmful chlorinated disinfection by-products. Further, flotation and coagulation are only able to transform pollutants from liquid into solid phase [3]. In recent decades, the application of advanced oxidation processes (AOPs), as an acceptable and efficient method, has been attracting increased attention among researchers and plant operators [13].

Fenton process, which is one of the most common AOPs, is based on the production of hydroxyl radicals ($OH^•$) as a result of the reaction between H_2O_2 and Fe^{2+} under acidic conditions [14]. In the process, Fe^{2+} is rapidly converted to Fe^{3+} reacting with H_2O_2 much more slowly than Fe^{2+}. Moreover, Fe^{3+} changes slowly into Fe^{2+}. Also, in Fenton reactions, the conversion of Fe^{3+} into Fe^{2+} is very slow. Therefore, the efficiency of the Fenton reaction slows down over time. But, on the other hand, the amount of chemical treatment sludge can increase as a result of continuous release of Fe^{2+} [15]. However, in order to accelerate the conversion of Fe^{3+} into Fe^{2+}, the sono-Fenton process ($US/H_2O_2/Fe^{2+}$) can be used. Thus, the H_2O_2 concentrations necessary for the reaction may also be reduced [16]. The main mechanism of US in the oxidation of the pollutants is formation of micro-bubbles [17], which develop through acoustic cavitation in water that create localized areas known as Hot Spot with temperatures as high as 5,000 K and pressures as high as 1,000 atm resulting in generation of $OOH^•$, $OH^•$, $H^•$, and $O^•$ radicals around the bubbles [18].

Ninomiya et al. [19] used sonocatalytic–Fenton reaction to degrade lignin and found that the degradation percentages of US individually, Fenton, and Sono-Fenton were, respectively, 2%, 20%, and 60% after 180 min [19]. In recent years, persulfate ($S_2O_8^{2-}$) has drawn increasing attention as a strong oxidizing agent (E^0 = 2.01 V). It offers some advantages over other oxidants as a relatively cheap chemical, nonselectivity in degradation of organic pollutants, high stability of generated radicals, high aqueous solubility, and a solid chemical at ambient temperature with the ease of storage and transport [20]. Besides these benefits, many studies have shown that $S_2O_8^{2-}$ has a low oxidative ability to degrade organic materials at room temperature. Therefore, it is necessary to activate $S_2O_8^{2-}$ in order to enhance its oxidation potential. The activation of $S_2O_8^{2-}$, as an AOP, can be done by heat, UV light, transition metal ions (Me^{n+}), which can form the sulfate radical ($SO_4^{-•}$) with a high oxidation potential of 2.6 V [21,22]. Among the transition metals, Fe^{2+} has widely been used to activate $S_2O_8^{2-}$. However, there are some critical barriers in the application of Fe^{2+} including the requirement for high contents of Fe^{2+}, generation of a large amount of iron sludge, precipitation of Fe^{2+} as Fe^{3+} after reaction with $S_2O_8^{2-}$, and consumption of $SO_4^{-•}$ radicals at high concentrations [23]. It was also reported that US could accelerate persulfate to generate $SO_4^{-•}$ in $US/S_2O_8^{2-}/Fe^{2+}$ process.

A study by Wang et al. [24] on the degradation of Acid Orange 7 by $US/S_2O_8^{2-}/Fe^0$ confirmed that the optimum pH value could be achieved at 5.8. By considering the advantages and specific features of AOPs and US in the degradation of organic compounds especially dyes, the present study aimed to evaluate the effectiveness of $US/H_2O_2/Fe^{2+}$ and $US/S_2O_8^{2-}/Fe^{2+}$ on the decomposition of Acid Blue 113 (AB113). The effects of system variables such as initial solution pH, Fe^{2+} concentration, H_2O_2 concentration, $S_2O_8^{2-}$ concentration, and initial AB113 concentration were also investigated.

2. Materials and methods

2.1. Reagents

Hydrogen peroxide (purity 30%), sodium hydroxide, sulfuric acid, sulfate ferrous, and potassium persulfate were purchased from Merck (Germany). AB113 was bought from Alvansabet Co., Hamadan, Iran. Table 1 presents the characteristics of Acid Blue 113 in the dye. A digital ultrasound generator (model LUC-405) and spectrophotometer (DR5000, HACH) were used in the experiments.

2.2. Experimental setup

All experiments were performed in a 1,250-mL batch reactor (plexiglass) [25] containing 1,000 mL of the sample immersed in a water bath to keep the temperature at 25°C [19]. In addition to temperature adjustment by the ultrasound device, cold water was fed into the reactor, and warm water was let out. Then, it was operated at 40 kHz and an emission power of 350 W, stirred at a rate of 100 rpm [26].

The schematic diagram of the experimental setup employed in this study has been displayed in Fig. 1. In order to

Table 1
Characteristics of Acid Blue 113

Name	Acid Blue 113
Molecular structure	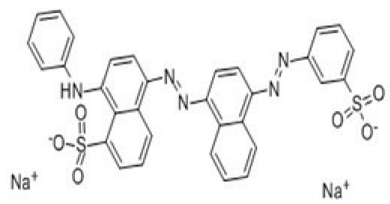
Molecular formula	$C_{32}H_{21}N_5Na_2O_6S_2$
Molecular weight	681.65 g/mol
Alternative name	Acid Fast Blue 5R

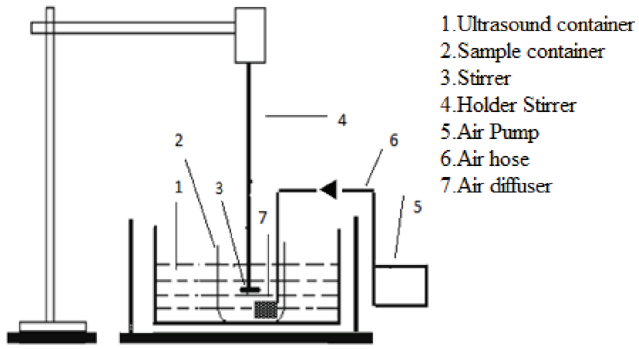

Fig. 1. Schematic diagram of the experimental setup employed in this study.

investigate the effect of aeration on the samples, a pump with a capacity of 3.5 L/min was used. The absorbance of the lignin solution was measured at a wavelength range of 190–700 nm to determine the concentration of lignin. To explore the changes of UV–Vis spectra of the dye under optimum conditions, wavelengths were scanned from 190 to 690 nm. Quartz sleeves were used to scan the wavelength range.

2.2.1. Effect of initial pH

In order to investigate the effect of pH range (3–11), solutions with fixed concentration of H_2O_2 = 2.5 mM, $S_2O_8^{2-}$ = 2.5 mM, and AB113 = 50 mg/L were prepared. Sampling was done after 45 min of the reaction. Sodium hydroxide 1 N and sulfuric acid 1 N were used to adjust the pH values of the samples.

2.2.2. Effect of Fe^{2+} concentration

In order to study the impact of Fe^{2+} concentration on the removal efficiency, some runs were conducted under the following conditions: Fe^{2+} concentration 0.01–1 mM, pH 3, H_2O_2 = 2.5 mM, $S_2O_8^{2-}$ = 2.5 mM, AB113 = 50 mg/L, and reaction time 45 min.

2.2.3. Effect of H_2O_2 and $S_2O_8^{2-}$ concentration

In order to study the impact of concentrations of H_2O_2 and $S_2O_8^{2-}$on the performance, some experiments were carried out under the following conditions: H_2O_2 concentration 1–10 mM, $S_2O_8^{2-}$ concentration 1–10 mM, Fe^{2+} 0.05 mM, and AB113 50 mg/L in a batch manner.

2.2.4. Effect of initial AB113 dye concentration

So as to investigate the effect of initial AB113 concentration on the decolorization effectiveness, experiments were done under the conditions as follows: dye content 25–200 mg/L, H_2O_2 concentration 2.5 mM, $S_2O_8^{2-}$ 2.5 mM, Fe^{2+} 0.05 mM, pH 3, and reaction time 45 min.

2.2.5. Effects of aeration

In order to study the effect of aeration in the processes: US/H_2O_2/Fe^{2+} and US/$S_2O_8^{2-}$/Fe^{2+}, the removal efficiency was performed under the optimum conditions with aeration rate of 3 L/min and at reaction time of 0–45 min. Also, the impact of aeration on the efficiency of sole ultrasound waves for removing AB113 dye was examined at reaction time of 0–45 min.

2.2.6. Effects of ultrasound waves and synergistic impact of the parameters

To examine the sole and combined effects of ultrasound waves, the optimum value of the effective factors on the process was used, and the samples were collected at 45th minute.

2.3. Analysis of Acid Blue 113

The residual concentrations of the dye in aqueous solutions were determined at an absorption wavelength of 478 nm. For this wavelength, an appropriate amount of the dye was prepared at pH 7. Color changes were determined by a UV–Vis spectrophotometer (DR5000) and in quartz cuvettes at a wavelength range from 190 to 700 nm. The absorption peak occurred at a wavelength of 567 nm. To explore the effect of pH on the wavelength range, all these steps were repeated for the samples with pH 3 and 11 (Fig. 2). Wavelength scan showed that any change in pH value changes or reduces the peak values (i.e., acidic and basic pH, respectively, decreases and increases the peak). Thus, the pH of all the samples was fixed at 7 before the measurement. The results of the scan have been summarized in Table 1. In this study, a standard curve was used to calculate the amounts of absorbance as concentration in mg/L.

3. Results and discussion

3.1. Effect of initial pH

The effect of pH on the degradation rate of AB113 has been shown in Fig. 3. The highest removal efficiencies (93.5% and 94.3%) were achieved, respectively, for US/H_2O_2/Fe^{2+} and US/$S_2O_8^{2-}$/Fe^{2+} at pH 3. The results illustrated that the decolorization efficiency decreased significantly with increasing pH.

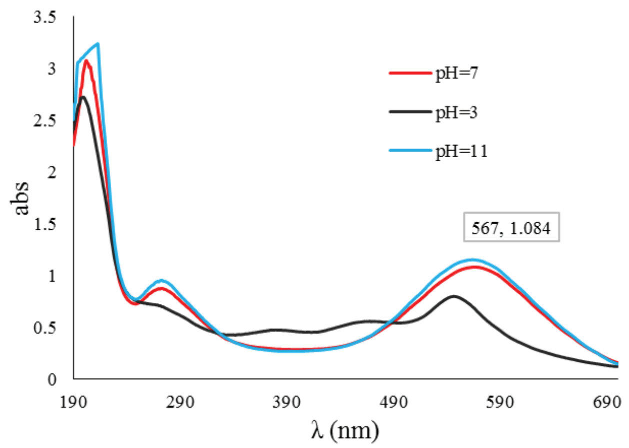

Fig. 2. Wavelength scan of AB113 at concentration of 50 mg/L and pHs 3, 7 and 11.

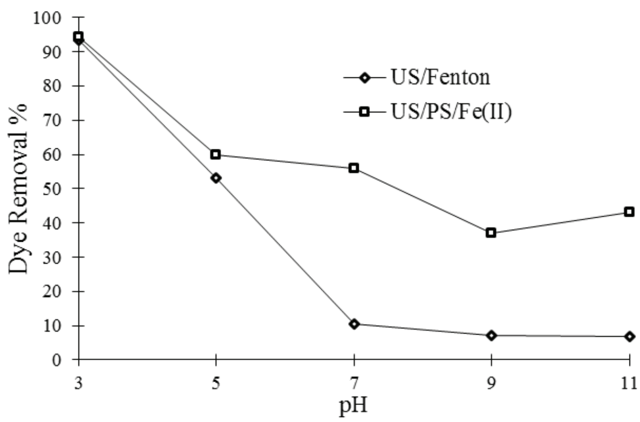

Fig. 3. Effect of pH on the degradation efficiency of AB113 by US/H_2O_2/Fe^{2+} and US/$S_2O_8^{2-}$/Fe^{2+} (experimental conditions: H_2O_2 = 2.5 mM, $S_2O_8^{2-}$ = 2.5 mM, ferrous sulfate = 0.05 mM, AB113 = 50 mg/L, reaction time = 45 min, US irradiation = 40 kHz).

As can be seen, the US/H_2O_2/Fe^{2+} process showed a better performance as compared with the other process. For example, the removal efficiencies for the two processes were 7% and 43%, respectively, at pH 11.

Other studies have shown that solution pH is one of the main factors affecting the removal efficiency in chemical processes. In AOPs, pH has a direct effect on the stability of H_2O_2, generation of $OH^•$ radicals and the phase of iron in the solution. Compared with other similar studies, the results demonstrated that the Fenton and Fenton-like processes have the highest efficiency in acidic conditions in the range of 2–4 [15,18]. Eq. (1) shows the Fenton's reaction in the solution [14]:

$$Fe^{2+} + H_2O_2 \rightarrow Fe^{3+} + OH^- + OH^• \quad (1)$$

In Fenton process, at pH > 5, H_2O_2 cannot stay stable and rapidly dissociates into H_2O and O_2. However, the oxidation potential of $OH^•$ may decrease with increasing pH. The efficiency of the Fenton and Fenton-like processes decreases significantly when the pH in solution rises [27]. At pH above 4 in Fenton process, Fe^{2+} precipitated as iron hydroxides (Fe^{3+}), which suppressed the catalytic activity for H_2O_2 and lowered regeneration of hydroxyl radicals. Further increase of pH level caused the precipitation of Fe^{3+} into $Fe(OH)_3$, thereby decreasing the amounts of sludge produced. Iron only participates in reactions when it exists in solution in dissolved phase as shown in Eq. (2) [17]:

$$Fe^{2+} + H_2O \rightarrow FeOH^+ + H^+ \quad (2)$$

$S_2O_8^{2-}$/Fe^{2+} exhibits reactions similar to that of Fenton's regent in terms of iron phase [28,29]. Also, at pH > 9, $FeOH^{3+}$, $Fe(OH)_4^-$, $Fe(OH)_3^•$, and $Fe_2(OH)_3^{4+}$ species were formed that have low efficiency to activate persulfate to produce the sulfate radicals [30]. Activation of $S_2O_8^{2-}$ by Fe^{2+} forming SO_4^- can be slightly changed by changing pH value and tend the reaction toward the generation of $OH^•$; this reaction occurs better at basic pH values (Eqs. (4) and (5)).

Thus, the main species of the $S_2O_8^{2-}$/Fe^{2+} process is highly pH dependent, and at pH < 7 (especially at 3–5) $SO_4^{-•}$ is the predominant product (Eq. (3)). Both radicals are present in the solution at pH values between 7 and 9 (Eq. (4)). Under highly alkaline environments (especially pH > 12), $OH^•$ radicals are predominant (Eq. (5)).

Since the oxidation potential of the $OH^•$ radical decreases significantly under basic conditions, the degradation efficiency decreases even in the presence of this radical. The stability of $SO_4^{-•}$ radicals is higher than that of $OH^•$ radicals in aqueous environments [31].

$$S_2O_8^{2-} + Fe^{2+} \rightarrow SO_4^{•-} + Fe^{3+} + SO_4^{2-} \quad (3)$$

$$SO_4^{•-} + H_2O \leftrightarrow OH^• + H^+ + SO_4^{2-} \quad (4)$$

$$SO_4^{•-} + OH^- \rightarrow OH^• + SO_4^{2-} \quad (5)$$

Chen and Huang [32] reported that the pH value for mineralizing aniline through electrical activation of persulfate in the presence of UV waves was 3. Moreover, Rao et al. [33] also degraded carbamazepine by the $S_2O_8^{2-}$/Fe^{2+} process.

3.2. Effect of Fe^{2+} concentration

The effect of Fe^{2+} concentration ranging from 0.01 to 1 on AB113 degradation was examined (Fig. 4). The results showed that an increase in Fe^{2+} concentration, as the source of Fe^{2+}, from 0.01 to 0.5 mM accelerated the degradation efficiency of US/H_2O_2/Fe^{2+} and US/$S_2O_8^{2-}$/Fe^{2+}, which reached to 98% and 99.9% from 74% and 91%, respectively. It was also found that a further increase in Fe^{2+} concentration up to 1 mM resulted in a decrease in decolorization rate of the both processes.

The reason for the effect of iron concentration in the reaction is that H_2O_2 requires Fe^{2+} ions in order to generate $OH^•$ radicals (Eq. (1)). In comparison with Fe^{3+}, Fe^{2+} can better catalyze H_2O_2 and generate $OH^•$ radicals.

Based on Eq. (6), the chemical reaction between H_2O_2 and Fe^{3+} would result in the generation of $OOH^•$ radicals, which react slowly with organic contaminants.

However, in Fenton process, self-quenching reactions are likely to occur, especially if there is an excess of Fe^{2+} concentration in the solution (Eq. (7)), a further decrease in the efficiency due to the consumption of $OH^•$ by Fe^{2+} and more production of Fe^{3+} [34,35] is expected to happen.

$$Fe^{3+} + H_2O_2 \rightarrow Fe^{2+} + H^+ + OOH^• \quad (6)$$

$$Fe^{2+} + OH^• \rightarrow Fe^{3+} + OH^- \quad (7)$$

However, more increase of Fe^{3+} concentration causes can result in the production of $Fe(HO_2)^{2+}$ (Eq. (8)), as a by-product, which can be slowly converted into Fe^{2+} ions and $OOH^•$ radicals. In US/H_2O_2/Fe^{2+} process, US irradiation can enhance this reaction leading to the increased removal efficiency. The generated Fe^{2+} reacts with H_2O_2 and increases the overall removal efficiency according to Eq. (9) [36,37].

$$Fe^{3+} + H_2O_2 \rightarrow Fe\text{-}O_2H^{2+} + H^+ \quad (8)$$

$$Fe\text{-}O_2H^{2+} +))) \rightarrow Fe^{2+} + OOH^• \quad (9)$$

The $S_2O_8^{2-}$/Fe^{2+} process exhibits reactions similar to those of Fenton's regent in terms of iron phase. Further increase of

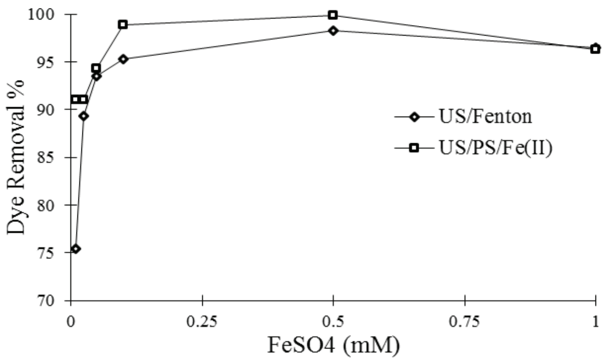

Fig. 4. Effect of ferrous sulfate concentration on the degradation efficiency of AB113 by US/H_2O_2/Fe^{2+} and US/$S_2O_8^{2-}$/Fe^{2+} (experimental conditions: H_2O_2 = 2.5 mM, $S_2O_8^{2-}$ = 2.5 mM, pH = 3, AB113 = 50 mg/L, reaction time = 45 min, US irradiation = 40 kHz).

Fe^{2+} from a particular amount not only decreases the removal efficiency of the system but also causes more sludge production that decreases the overall decolorization rate due to $SO_4^{-\bullet}$ radicals attraction by Fe^{2+} in accordance with Eq. (10) [38]. In this study, the removal efficiency of both processes decreased with increasing Fe^{2+} concentration above 0.5 mM.

$$SO_4^{\bullet -} + Fe^{2+} \rightarrow SO_4^{2-} + Fe^{3+} \quad (10)$$

3.3. Effect of H_2O_2 and $S_2O_8^{2-}$ on decolorization efficiency

The results indicated that an increase in H_2O_2 and $S_2O_8^{2-}$ concentration from 1 to 10 mM increased the removal efficiency of AB113 to some extent in both $US/H_2O_2/Fe^{2+}$ and $US/S_2O_8^{2}/Fe^{2+}$ processes, but further increase beyond this level decreased the efficiency (Fig. 5). The maximum decolorization efficiencies in the highest amount of the applied oxidant were 99.6% and 95.6% for the both processes, respectively.

The reason is that H_2O_2 acts as an oxidant in Fenton and Fenton-related processes, and by raising its concentration, more OH radicals were produced, thereby increasing the decolorization rate [39]. With respect to $S_2O_8^{2-}$ concentration, further increase of oxidant concentration from a particular amount not only decreases the removal efficiency of the process but also attracts $SO_4^{-\bullet}$ radicals from the aqueous environment, which overall declines the decolorization rate in accordance with Eq. (11) [40]. Therefore, 5 mM H_2O_2 and 2 mM $S_2O_8^{2}$ were selected as the optimum contents.

$$S_2O_8^{2-} + SO_4^{\bullet -} \rightarrow S_2O_8^{\bullet -} + SO_4^{2-} \quad (11)$$

3.4. Effect of initial AB113 concentration

The effects of initial concentration of AB113 on the degradation rate have been shown in Fig. 6. As can be seen from the figure, the removal efficiency decreased with increasing AB113 concentration from 25 to 200 mg/L for both processes. For example, the efficiency for $US/H_2O_2/Fe^{2+}$ and $US/S_2O_8^{2-}/Fe^{2+}$ was 57% and 68%, respectively, at the concentration of 200 mg/L.

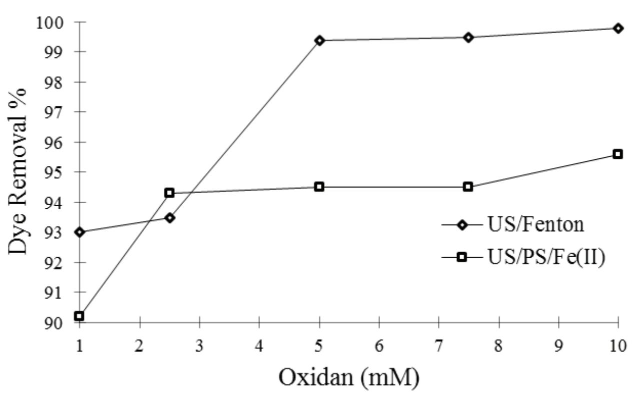

Fig. 5. Effect of H_2O_2 and $S_2O_8^{2-}$ on the degradation efficiency of AB113 by $US/H_2O_2/Fe^{2+}$ and $US/S_2O_8^{2-}/Fe^{2+}$ (experimental conditions: pH = 3, ferrous sulfate = 0.05 mM, AB113 = 50 mg/L, reaction time = 45 min, US irradiation = 40 kHz).

Various studies, in which the oxidation of organic compounds has been investigated, have reported that an increase in pollutant content decreases the process efficiency. This may be due to the abatement of ratio of generated radicals to the pollutant concentration. Another reason is attributed to the further generation of intermediates, which consume the available radicals [41].

3.5. Effect of aeration

In order to investigate the effects of aeration on the decolorization, air was injected into the reactor (Fig. 7). The removal efficiencies declined from 84% and 92% to 93.5% and 94.3%, respectively, for $US/H_2O_2/Fe^{2+}$ and $US/S_2O_8^{2-}/Fe^{2+}$ after 45 min of aeration. At the same reaction time in US process individually, aeration enhanced the removal efficiency from 6% to 11%.

By the propagation of ultrasonic waves into a nonchemical reactor, the water and oxygen molecules get excited and dissociated, and in turn, reactive species are generated in

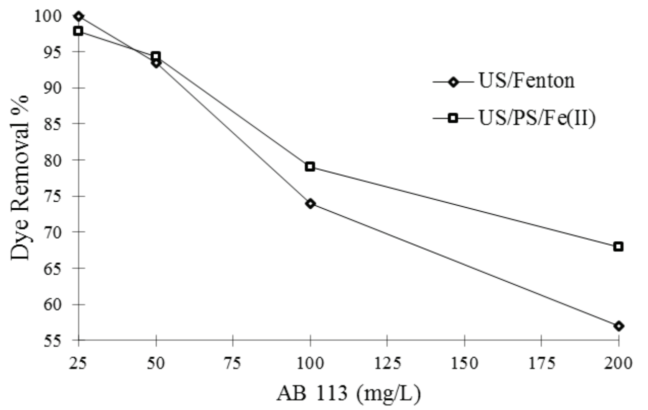

Fig. 6. Effect of AB113 on the process efficiency by $US/H_2O_2/Fe^{2+}$ and $US/S_2O_8^{2-}/Fe^{2+}$ (experimental conditions: H_2O_2 = 2.5 mM, $S_2O_8^{2-}$ = 2.5 mM, pH = 3, ferrous sulfate = 0.05 mM, reaction time = 45 min, US irradiation = 40 kHz).

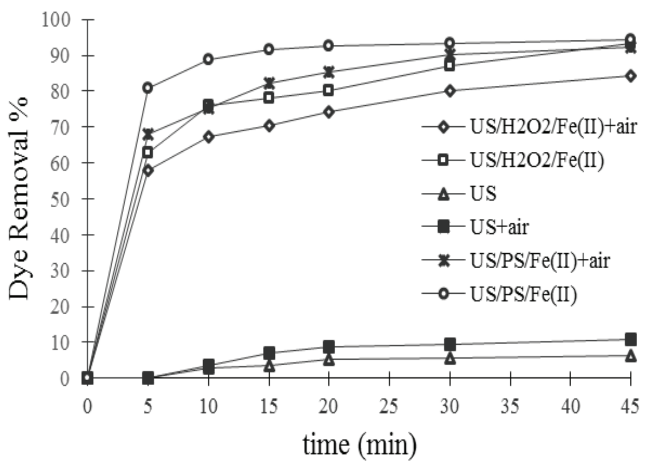

Fig. 7. Effect of aeration on the degradation efficiency of AB113 by $US/H_2O_2/Fe^{2+}$ and $US/S_2O_8^{2-}/Fe^{2+}$ (experimental conditions: H_2O_2 = 2.5 mM, $S_2O_8^{2-}$ = 2.5 mM, pH = 3, ferrous sulfate = 0.05 mM, AB113 = 50 mg/L, US irradiation = 40 kHz).

accordance with Eqs. (12) and (13). The introduction of ultrasound waves in an aqueous solution generates micro-bubbles that grow, pulsate, and collapse, and consequently lead to the formation of OH•, H•, and O• radicals [42]. After Eqs. (14) and (15), OOH• and OH• radicals are generated [43]. But in $US/H_2O_2/Fe^{2+}$ and $US/S_2O_8^{2-}/Fe^{2+}$ processes, due to the necessity of Fe^{2+} presence, aeration leads to the oxidation of Fe^{2+} into Fe^{3+} forming $Fe(OH)_3$; as a result, a decrease in efficiency occurs since Fe^{3+} has a lower ability to active H_2O_2 and $S_2O_8^{2-}$ [42,43].

$$H_2O))) H^\bullet + OH^\bullet \quad (12)$$

$$O_2))) 2O^\bullet \quad (13)$$

$$O^\bullet + H_2O \rightarrow 2OH^\bullet \quad (14)$$

$$H^\bullet + O_2 \rightarrow OOH^\bullet \quad (15)$$

3.6. Effect of US irradiation and the synergistic effect

In order to investigate the role of each parameter on the removal efficiency, sampling was done after 45 min of reaction (Fig. 8). Fe^{2+}, US, $S_2O_8^{2-}$, and H_2O_2 yielded removal efficiencies of 2.6%, 6.2%, 14.5% and 39%, respectively, at initial concentration of 50 mg/L. The results also indicated that the combination of ultrasound as US/H_2O_2 and $US/S_2O_8^{2-}$ increased the removal efficiency to 58% and 28.4%, respectively.

Evidently, UV waves in concert with H_2O_2 had synergistic effect increasing 12.8% the removal efficiency more. This effect for the combination of US and $S_2O_8^{2-}$ was 7.7%. The synergetic effects observed in $US/H_2O_2/Fe^{2+}$ and $US/S_2O_8^{2-}/Fe^{2+}$ processes were 1.9% and 7.54%, respectively.

US waves, due to the ability to generate H_2O_2 directly in the solution, can simultaneously increase the process efficiency for both US and Fenton in accordance to Eqs. (16) and (18). Despite many benefits associated with the application of the US process in the purification of pollutants in water resources, as shown by the literature review, the efficiency of ultrasound waves is not considerable in removing contaminations [44,45] and since other. To overcome these disadvantages, various combined ultrasound treatment systems such as US/O_3, US/H_2O_2, electrochemical (US/electro-Fenton), Fenton's reagent, photocatalysts, and other catalytic oxidation processes have been studied [17]. Generally, results have shown that coupled ultrasound processes had better performance than ultrasound alone.

$$2OH^\bullet \rightarrow H_2O_2 \quad (16)$$

$$OH^\bullet + H_2O \rightarrow H_2O_2 \quad (17)$$

$$2H_2O^\bullet \rightarrow H_2O_2 \quad (18)$$

US waves are also able to convert required iron in Fenton and $S_2O_8^{2-}/Fe^{2+}$ into Fe^{3+} and then back into Fe^{2+} more rapidly [46].

3.7. Analysis of UV-Vis spectrum of AB113 absorbance

Variations in the wavelength scan of AB113 adsorption in $US/S_2O_8^{2-}/Fe^{2+}$ and $S_2O_8^{2-}/Fe^{2+}$ processes have been shown in Fig. 9. As can be seen from the figure, three peaks are observed at 567, 276, and 203 nm, which all charged as reaction proceeds. Among these, the peak at 567 nm shows the highest abatement, which is attributed to the azo bond. The highest change in the UV–Vis spectrum of AB113 is observed for $US/H_2O_2/Fe^{2+}$, $US/S_2O_8^{2-}/Fe^{2+}$, $S_2O_8^{2-}/Fe^{2+}$, and H_2O_2/Fe^{2+}.

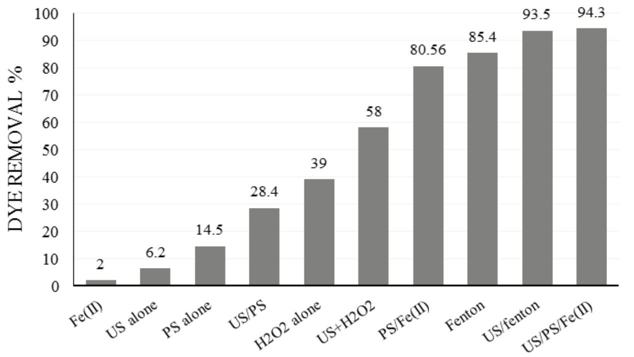

Fig. 8. Synergistic effects as a function of different parameters in this study (experimental conditions: H_2O_2 = 2.5 mM, $S_2O_8^{2-}$ = 2.5 mM, pH = 3, ferrous sulfate = 0.05 mM, AB113 = 50 mg/L, reaction time = 45 min, US irradiation = 40 kHz).

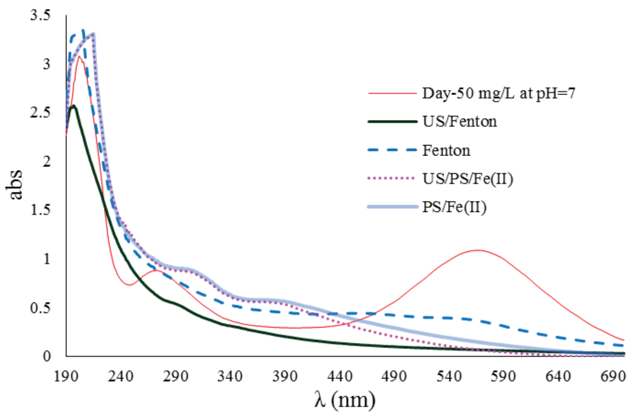

Fig. 9. UV–Vis spectral changes of AB113 under optimum conditions.

These results are consistent with the results reported by Sun et al. [47] who used the Fenton process facilitated by ultrasonic irradiation to degrade Acid Black 1. In Xu and Li [28] study, three peaks were observed on Orange G structure at 478, 328, and 259 nm. While the peaks at 259 and 328 nm are assigned to its aromatic rings, the peak at 478 nm and the shoulder peak at 421 nm are assigned to the conjugated structure formed by the azo bond. In the present study, the absorption peaks of the azo bond in $S_2O_8^{2-}/Fe^{2+}$ process also declined more slowly compared with that of aromatic rings.

4. Conclusion

The results of the present study showed that AB113 degradation yields best under acidic conditions for both $US/H_2O_2/Fe^{2+}$ and $US/S_2O_8^{2-}/Fe^{2+}$. At Fe^{2+} concentration >5 mM, the decolorization efficiency decreased for the both processes. An increase in H_2O_2 and $S_2O_8^{2-}$concentrations increased the degradation rate. Aeration in the sonochemical reactor individually increased the decolorization rate. The highest change in the UV–Vis spectrum of AB113 absorbance is assigned to US/H_2O_2/Fe^{2+}.

References

[1] A. Karimi, F. Mahdizadeh, M. Eskandarian, Enzymatic in-situ generation of H_2O_2 for decolorization of Acid Blue 113 by Fenton process, Chem. Ind. Chem. Eng. Q., 18 (2012) 89–94.

[2] R. Khosravi, M. Fazlzadehdavil, B. Barikbin, H. Hossini, Electro-decolorization of Reactive Red 198 from aqueous solutions using aluminum electrodes systems: modeling and optimization of operating parameters, Desal. Wat. Treat., 54 (2015) 3152–3160.

[3] A.R. Rahmani, A. Shabanloo, M. Fazlzadeh, Y. Poureshgh, Investigation of operational parameters influencing in treatment of dye from water by electro-Fenton process, Desal. Wat. Treat., 57 (2016) 24387–24394.

[4] M. Fazlzadeh, H. Abdoallahzadeh, R. Khosravi, B. Alizadeh, Removal of acid black 1 from aqueous solutions using Fe_3O_4 magnetic nanoparticles, J. Mazandaran Univ. Med. Sci., 26 (2015) 174–186.

[5] A.H. Movahedian, R. Rezaei, Investigating the efficiency of advanced photochemical oxidation (APO) technology in degradation of direct azo dye by UV/H_2O_2 process, J. Water Wastewater, 59 (2006) 75–83.

[6] M.M. Ghoneim, H.S. El-Desoky, N.M. Zidan, Electro-Fenton oxidation of Sunset Yellow FCF azo-dye in aqueous solutions, Desalination, 274 (2011) 22–30.

[7] B. Krishnakumar, M. Swaminathan, Solar photocatalytic degradation of Acid Black 1 with ZnO, Indian J. Chem., Sect. A, 49 (2010) 1035–1040.

[8] R. Khosravi, S. Hazrati, M. Fazlzadeh, Decolorization of AR18 dye solution by electrocoagulation: sludge production and electrode loss in different current densities, Desal. Wat. Treat., 57 (2016) 14656–14664.

[9] A. Rahmani, A. Shabanloo, M. Fazlzadeh, Y. Poureshgh, H. Rezaeivahidian, Degradation of Acid Blue 113 in aqueous solutions by the electrochemical advanced oxidation in the presence of persulfate, Desal. Wat. Treat., 59 (2017) 202–209.

[10] M. Pirsaheb, A. Dargahi, S. Hazrati, M. Fazlzadehdavil, Removal of diazinon and 2,4-dichlorophenoxyacetic acid (2,4-D) from aqueous solutions by granular-activated carbon, Desal. Wat. Treat., 52 (2014) 4350–4355.

[11] R. Khosravi, M. Fazlzadehdavil, B. Barikbin, A.A. Taghizadeh, Removal of hexavalent chromium from aqueous solution by granular and powdered Peganum Harmala, Appl. Surf. Sci., 292 (2014) 670–677.

[12] H. Abdoallahzadeh, B. Alizadeh, R. Khosravi, M. Fazlzadeh, Efficiency of EDTA modified nanoclay in removal of humic acid from aquatic solutions, J. Mazandaran Univ. Med. Sci., 26 (2016) 111–125.

[13] S. Parastar, S. Nasseri, S.H. Borji, M. Fazlzadeh, A.H. Mahvi, A.H. Javadi, M. Gholami, Application of Ag-doped TiO_2 nanoparticle prepared by photodeposition method for nitrate photocatalytic removal from aqueous solutions, Desal. Wat. Treat., 51 (2013) 7137–7144.

[14] A. Safarzadeh-Amiri, J.R. Bolton, S.R. Cater, The use of iron in advanced oxidation processes, J. Adv. Oxid. Technol., 1 (1996) 18–26.

[15] C. Özdemir, M.K. Öden, S. Şahinkaya, E. Kalipçi, Color removal from synthetic textile wastewater by sono-fenton process, Clean, 39 (2011) 60–67.

[16] J.T. Li, Y.L. Song, Degradation of AR 97 aqueous solution by combination of ultrasound and Fenton reagent, Environ. Prog. Sustain. Energy, 29 (2010) 101–106.

[17] Y. Li, W.-P. Hsieh, R. Mahmudov, X. Wei, C. Huang, Combined ultrasound and Fenton (US-Fenton) process for the treatment of ammunition wastewater, J. Hazard. Mater., 244 (2013) 403–411.

[18] A.S. Mohammadi, H.M. Attar, *p*-Chlorophenol oxidation in industrial effluent by ultrasonic/Fenton technology, Water Wastewater, 22 (2011) 43–49.

[19] K. Ninomiya, H. Takamatsu, A. Onishi, K. Takahashi, N. Shimizu, Sonocatalytic–Fenton reaction for enhanced OH radical generation and its application to lignin degradation, Ultrason. Sonochem., 20 (2013) 1092–1097.

[20] G. Asgari, A. Chavoshani, A. Seid-Mohammadi, A. Rahmani, Removal of pentachlorophenol using microwave assisted persulfate from synthetic wastewater, J. Water Wastewater, 25 (2013) 29–37.

[21] S.-Y. Oh, S.-G. Kang, D.-W. Kim, P.C. Chiu, Degradation of 2,4-dinitrotoluene by persulfate activated with iron sulfides, Chem. Eng. J., 172 (2011) 641–646.

[22] A. Ghauch, G. Ayoub, S. Naim, Degradation of sulfamethoxazole by persulfate assisted micrometric Fe_0 in aqueous solution, Chem. Eng. J., 228 (2013) 1168–1181.

[23] S.-Y. Oh, S.-G. Kang, P.C. Chiu, Degradation of 2,4-dinitrotoluene by persulfate activated with zero-valent iron, Sci. Total Environ., 408 (2010) 3464–3468.

[24] X. Wang, L. Wang, J. Li, J. Qiu, C. Cai, H. Zhang, Degradation of Acid Orange 7 by persulfate activated with zero valent iron in the presence of ultrasonic irradiation, Sep. Purif. Technol., 122 (2014) 41–46.

[25] M.R. Samaei, H. Maleknia, A. Azhdarpoor, A comparative study of removal of methyl tertiary-butyl ether (MTBE) from aquatic environments through advanced oxidation methods of H_2O_2/nZVI, H_2O_2/nZVI/ultrasound, and H_2O_2/nZVI/UV, Desal. Wat. Treat., 57 (2016) 21417–21427.

[26] L. Hou, H. Zhang, X. Xue, Ultrasound enhanced heterogeneous activation of peroxydisulfate by magnetite catalyst for the degradation of tetracycline in water, Sep. Purif. Technol., 84 (2012) 147–152.

[27] H. Shemer, K.G. Linden, Degradation and by-product formation of diazinon in water during UV and UV/H_2O_2 treatment, J. Hazard. Mater., 136 (2006) 553–559.

[28] X.-R. Xu, X.-Z. Li, Degradation of azo dye Orange G in aqueous solutions by persulfate with ferrous ion, Sep. Purif. Technol., 72 (2010) 105–111.

[29] N. Masomboon, C. Ratanatamskul, M.-C. Lu, Chemical oxidation of 2,6-dimethylaniline by electrochemically generated Fenton's reagent, J. Hazard. Mater., 176 (2010) 92–98.

[30] L. Zhou, W. Zheng, Y. Ji, J. Zhang, C. Zeng, Y. Zhang, Q. Wang, X. Yang, Ferrous-activated persulfate oxidation of arsenic(III) and diuron in aquatic system, J. Hazard. Mater., 263 (2013) 422–430.

[31] A. Romero, A. Santos, F. Vicente, C. González, Diuron abatement using activated persulphate: effect of pH, Fe(II) and oxidant dosage, Chem. Eng. J., 162 (2010) 257–265.

[32] W.-S. Chen, C.-P. Huang, Mineralization of aniline in aqueous solution by electro-activated persulfate oxidation enhanced with ultrasound, Chem. Eng. J., 266 (2015) 279–288.

[33] Y. Rao, L. Qu, H. Yang, W. Chu, Degradation of carbamazepine by Fe(II)-activated persulfate process, J. Hazard. Mater., 268 (2014) 23–32.

[34] H. Ghodbane, O. Hamdaoui, Degradation of Acid Blue 25 in aqueous media using 1700 kHz ultrasonic irradiation: ultrasound/Fe(II) and ultrasound/H_2O_2 combinations, Ultrason. Sonochem., 16 (2009) 593–598.

[35] X. Wang, Z. Yao, J. Wang, W. Guo, G. Li, Degradation of reactive brilliant red in aqueous solution by ultrasonic cavitation, Ultrason. Sonochem., 15 (2008) 43–48.

[36] J. Liang, S. Komarov, N. Hayashi, E. Kasai, Improvement in sonochemical degradation of 4-chlorophenol by combined use of Fenton-like reagents, Ultrason. Sonochem., 14 (2007) 201–207.

[37] M. Muruganandham, J.-S. Yang, J.J. Wu, Effect of ultrasonic irradiation on the catalytic activity and stability of goethite catalyst in the presence of H_2O_2 at acidic medium, Ind. Eng. Chem. Res., 46 (2007) 691–698.

[38] S. Rodriguez, L. Vasquez, D. Costa, A. Romero, A. Santos, Oxidation of Orange G by persulfate activated by Fe(II), Fe(III) and zero valent iron (ZVI), Chemosphere, 101 (2014) 86–92.

[39] C.-H. Weng, Y.-T. Lin, H.-M. Yuan, Rapid decoloration of Reactive Black 5 by an advanced Fenton process in conjunction with ultrasound, Sep. Purif. Technol., 117 (2013) 75–82.
[40] C. Liang, Z.-S. Wang, C.J. Bruell, Influence of pH on persulfate oxidation of TCE at ambient temperatures, Chemosphere, 66 (2007) 106–113.
[41] J. Wu, H. Zhang, J. Qiu, Degradation of Acid Orange 7 in aqueous solution by a novel electro/Fe^{2+}/peroxydisulfate process, J. Hazard. Mater., 215 (2012) 138–145.
[42] F. Chen, Y. Li, W. Cai, J. Zhang, Preparation and sono-Fenton performance of 4A-zeolite supported α-Fe_2O_3, J. Hazard. Mater., 177 (2010) 743–749.
[43] V. Naddeo, V. Belgiorno, D. Kassinos, D. Mantzavinos, S. Meric, Ultrasonic degradation, mineralization and detoxification of diclofenac in water: optimization of operating parameters, Ultrason. Sonochem., 17 (2010) 179–185.
[44] M.R. Doosti, R. Kargar, M.H. Sayadi, Water treatment using ultrasonic assistance: a review, Proc. Inter. Acad. Ecol. Environ. Scie., 2 (2012) 96–110.
[45] M. Dükkancı, M. Vinatoru, T.J. Mason, The sonochemical decolourisation of textile azo dye Orange II: effects of Fenton type reagents and UV light, Ultrason. Sonochem., 21 (2014) 846–853.
[46] Y.L. Pang, A.Z. Abdullah, S. Bhatia, Review on sonochemical methods in the presence of catalysts and chemical additives for treatment of organic pollutants in wastewater, Desalination, 277 (2011) 1–14.
[47] J.-H. Sun, S.-P. Sun, J.-Y. Sun, R.-X. Sun, L.-P. Qiao, H.-Q. Guo, M.-H. Fan, Degradation of azo dye Acid black 1 using low concentration iron of Fenton process facilitated by ultrasonic irradiation, Ultrason. Sonochem., 14 (2007) 761–766.